Chin Med Sci J
September 2019

Vol. 34, No. 3 P. 168-176
doi:10.24920/003585

ORIGINAL ARTICLE

Identification of CDK6 and RHOU in Serum Exosome as Biomarkers for the Invasiveness of Non-functioning Pituitary Adenoma

Shan Yu[1], Xiaoshuang Wang[1], Kaican Cao[2], Xinjie Bao[3]*, Jia Yu[1]*

[1]State Key Laboratory of Medical Molecular Biology & Key Laboratory of RNA and Hematopoietic Regulation & Department of Biochemistry, Institute of Basic Medical Sciences, Chinese Academy of Medical Sciences & School of Basic Medicine, Peking Union Medical College, Beijing 100005, China
[2]Department of Thoracic Surgery, Nanfang Hospital, Guangzhou 510515, China
[3]Department of Neurosurgery, Peking Union Medical College Hospital, Chinese Academy of Medical Sciences & Peking Union Medical College, Beijing 100730, China

Key words: pituitary adenoma; invasiveness; exosome; droplet digital PCR; biomarkers; RHOU; CDK6

Objective To explore circulating biomarkers for screening the invasiveness of non-functioning pituitary adenomas (NF-PAs).

Methods The exosomal RNAs were extracted from serum of patients with invasive NF-PA (INF-PA) or noninvasive NF-PA (NNF-PA). Droplet digital PCR was adapted to detect the mRNA expression of candidate genes related to tumor progression or invasion, such as cyclin dependent kinase 6 (CDK6), ras homolog family member U (RHOU), and spire type actin nucleation factor 2 (SPIRE2). Student's *t*-test was used to analyze the statistical difference in the mRNA expression of candidate genes between the two groups. Receiver operating characteristic (ROC) curve was used to establish a model for predicting the invasiveness of NF-PAs. The accuracy, sensitivity, specificity and precision of the model were then obtained to evaluate the diagnostic performance.

Received March 6, 2019. Published online May 22, 2019.

*Corresponding author Xinjie Bao, Tel: 86-18001182406, E-mail: xinjieabao@163.com; Jia Yu, Tel: 86-10-69156423, E-mail: j-yu@ibms.pumc.edu.cn

Supported by the National Natural Science Foundation of China (31725013), the CAMS Innovation Fund for Medical Sciences (2017-I2M-3-009), and the Beijing Nova Program (Z181100006218003).

Results CDK6 (0.2600±0.0912 *vs.* 0.1789±0.0628, $t=3.431$, $P=0.0013$) and RHOU mRNA expressions (0.2696±0.1118 *vs.* 0.1788±0.0857, $t=2.946$, $P=0.0052$) were upregulated in INF-PAs patients' serum exosomes as compared to NNF-PAs. For CDK6, the area under the ROC curve (AUC) was 0.772 (95% *CI*: 0.600-0.943, $P=0.005$), the accuracy, sensitivity, specificity and precision were 77.27%, 83.33%, 75.00% and 55.56% to predict the invasiveness of NF-PAs. For RHOU, the AUC was 0.757 (95% *CI*: 0.599-0.915, $P=0.007$), the accuracy, sensitivity, specificity and precision were 72.73%, 83.33%, 68.75% and 50.00%. In addition, the mRNA levels of CDK6 and RHOU in serum exosomes were significantly positively correlated ($r=0.935$, $P<0.001$). After combination of the cut-off scores of the two genes, the accuracy, sensitivity, specificity and precision were 81.82%, 83.33%, 81.25% and 62.50%.

Conclusions CDK6 and RHOU mRNA in serum exosomes can be used as markers for predicting invasiveness of NF-PAs. Combination of the two genes performs better in distinguishing INF-PAs from NNF-PAs. These results indicate CDK6 and RHOU play important roles in the invasiveness of NF-PAs, and the established diagnostic method is valuable for directing the clinical screening and postoperative treatment.

PITUITARY adenomas (PAs) are common neoplasms that originate from the adenohypophyseal cells, accounting for 10%-20% of intracranial neoplasms.[1, 2] Generally, PAs exhibit clinical manifestations due to excessive hormonal secretion, however, 30% PAs are clinically non-functioning (NF) with no evidence of hormone hypersecretion or no early symptoms until space occupying effect emerges.[3, 4] Most NF-PAs are non-invasive (NNF-PAs), which grow slowly, and some patients even need no excision and can carry the benign tumor for life-long time. In contrast, some NF-PAs (25%-55%) are invasive, which develop fast and could induce visual dysfunction, headache, hormone hyposecretion, or other neurological complications.[5] More importantly, invasive NF-PAs (INF-PAs) usually invade surrounding blood vessels, bones, sphenoid sinuses and optic chiasm, making them difficult to be resected and prone to relapse within three months.[6] Therefore, patients with INF-PAs relapse constantly or die even if they receive chemotherapy and radiotherapy after surgery.[7] Currently, it is very difficult to distinguish between NNF-PAs and INF-PAs due to the lacking of clinical guidelines, and the only diagnostic option is magnetic resonance imaging (MRI) examination. Thus, it is urgent to explore a novel diagnostic biomarker for predicting invasiveness of NF-PAs.

We had previously found a series of genes showing differential expression pattern in pituitaries between NNF-PA and INF-PA patients by high-throughput RNA-seq and further validated them by quantitative real-time PCR (qRT-PCR) in pituitary tissues (unpublished data). Furthermore, functional enrichment analysis suggested that pathways such as cell cycle and division were involved in tumor invasion. In order to protect the patients with NF-PAs and to predict invasiveness at early stage, we seek to search for circulating biomarkers in body fluids. Blood-brain barrier separates the circulating blood from brain while the adenohypophysis is not influenced, so the substances secreted by the pituitary gland and in blood can be exchanged freely. We then proposed that differentially expressed mRNA molecules in pituitary glands could show similar expression pattern in blood and might be used as diagnostic biomarkers.

One challenge for detecting circulating mRNAs is that they are extremely unstable and abundant ribonucleases exist in blood, however, exosomes are much more stable in body fluids. Exosomes are small vesicles (30-150 nm in diameter) derived from cells that can be detected in all fluids including blood.[8] Exosomes contain proteins and RNAs from their original cells and have been used for clinical diagnosis as well as predicting prognosis in various tumors.[9] Therefore, monitoring mRNAs in plasma or serum exosomes may provide robust circulating biomarkers. Since mRNA level in blood exosomes is fairly low, a unique technique called droplet digital PCR (ddPCR) with high sensitivity was adopted in this study.[10]

Among the highly expressed genes in INF-PAs, we focused on three candidates, cyclin dependent kinase 6 (CDK6), ras homolog family member U (RHOU), and spire type actin nucleation factor 2 (SPIRE2), based on their crucial function in tumors, and investigated their potentials as biomarkers for predicting invasiveness of NF-PAs. The mRNA levels of these genes were

analyzed in patients' serum exosomes by using ddPCR. According to the cut-off score, a diagnostic model for predicting the invasiveness of NF-PAs was finally established. Our results imply that CDK6 and RHOU could act as circulating biomarkers for screening INF-PAs.

MATERIALS AND METHODS

Patients and sample collection

Patients undergoing resection of NF-PAs at the Peking Union Medical College Hospital between April and November 2017 were eligible for the study. The diagnosis of NNF-PAs and INF-PAs was made according to MRI examination, intraoperative Knosp classification, combined with postoperative recurrence. In this study, NNF-PAs were defined as Knosp grade 0, 1, or 2, and importantly not involving the cavernous sinus. All INF-PAs were defined as Knosp grade 4 and involving the cavernous sinus definitely.[11] This study was approved by the ethical committee of Peking Union Medical College Hospital and all the participants were consent to participating in the analysis.

Exosome extraction from peripheral blood

The peripheral blood of each patient (about 5 ml) was taken in a Vacuette® tube (GREINER BIO-ONE, Germany). After incubated with serum separator clot activator at room temperature for 10 min, the blood sample was centrifuged at 1900 × *g*, 4°C for 10 min. The transferred supernatant was centrifugated at 1600 × *g* for 10 min at 4°C, and finally the cell-free supernatant was transferred into a new tube.

Exosomes were next extracted from 1 ml serum using Total Exosome Isolation Reagent (from serum) (Invitrogen, Waltham, MA, USA) according to the manufacturer's instructions. Approximately $(2.5\text{-}6.5) \times 10^{11}$ exosomes could be obtained from each sample. The pelleted exosomes were resuspended in PBS to examine exosome morphology using transmission electron microscopy with negative staining method and to display the size and quantity of the exosomes using nanoparticle tracking analysis with NanoSight NS300 instrument (Malvern Panalytical, England).

Exosomal RNA purification and reverse transcription

For total RNA extraction, the exosome pellet was lysed with 1 ml QIAzol Lysis Reagent (QIAGEN BIO-ONE), and proceeded using miRNeasy Micro Kit (QIAGEN B10-ONE). Then aliquots (11 μl) from total RNA were reverse transcribed using SuperScript™ Ⅲ Reverse Transcriptase (Invitrogen) following the manufacturer's instructions.

ddPCR

The ddPCR was performed following the recommendations of the supplier (Bio-Rad, California, USA). The reaction system contained 1 × ddPCR™ Supermix for Probes (no dUTP) (Bio-Rad), 800 nmol/L primer, 250 nmol/L probe (**Table 1**) and 3 μl of cDNA template in each 20 μl reaction system. After homogenization, the 20 μl ddPCR reaction mixture and 70 μl oil (Bio-Rad) were loaded into a droplet generator cartridge (Bio-Rad) to produce an emulsion about 40 μl in volume by QX200™ Droplet Generator. The emulsion was subsequently transferred to a 96-well PCR plate, heat-sealed by a pierceable foil (Bio-Rad) and subjected to thermal cycling under the following conditions: 95°C for 5 min for Taq polymerase activation; 40 cycles of 94°C for 30 s and 60°C for 40 s; then 98°C for 10 min and holding at 12°C. After amplification, the fluorescence intensity was read on a QX200 droplet reader. The result was analyzed with QuantaSoft software[12] (version 1.7.4.0917).

Functional enrichment

Functional enrichment analysis was carried out with KOBAS 3.0 and GSEA online. Gene IDs of the interested genes were submitted on KOBAS (http://kobas.cbi.pku.edu.cn/anno_iden.php) with all available database selected. For GSEA enrichment, gene sets were searched in Molecular Signatures Database (http://software.broadinstitute.org/gsea/msigdb/index.jsp).

Statistical analysis

Continuous data were expressed as mean ± SD. Statistical differences were analyzed by Student's *t*-test, *Chi-square* test or *Fisher* test using GraphPad Prism (version 6.0). A two-tailed *P* value less than 0.05 was considered as statistically significant. Receiver operating characteristic (ROC) curves and correlation analysis were depicted by IBM SPSS Statistics (version 22.0). ROC curves were used to assess the diagnosing accuracy for differentiating INF-PAs from NNF-PAs. The relative expression value of candidate exosomal mRNA corresponding to the Youden index (sensitivity + specificity -1) was defined as the cut-off score. The area

Table 1. Primers and probes for the target and reference genes

Gene name	Gene ID	Forward primer (5′-3′)	Reverse primer (5′-3′)	Probe (5′-3′)	Amplicon size (bp)
CDK6	1021	CTAGCAACCATCCCTCCATTAC	CTCAGAGCATTCTGAAGACAGTAG	ACACAGAAAGCCCTCTTGAAGCAA	104
RHOU	58480	GCAGGGAGGTGAATACTCTTG	GAAGTACATCTTGGCCGACTTA	AAGGCCAACAGCAAGTGTTTGTGGGA	92
SPIRE2	84501	GTCTGCACTTCCTGTAGCATAA	GATACCCTCTGAGGACTCTCAA	CACATCCCTGTCTACACACTGGGC	98
GAPDH	2597	GGTGTGAACCATGAGAAGTATGA	GAGTCCTTCCACGATACCAAAG	AGATCATCAGCAATGCCTCCTGCA	123

under ROC curve (AUC) was calculated to evaluate the diagnostic efficiency.

RESULTS

Clinical features of NNF-PA and INF-PA patients

Finally, 46 patients were recruited in the study, including 32 NNF-PAs and 14 INF-PAs. No significant difference in clinical features was observed between the NNF-PAs and INF-PAs groups except for tumor size ($t=3.7152$, $P=0.0006$; **Table 2**), which was consistent with the common knowledge that invasive PAs are larger than non-invasive ones at diagnosis. It should be noticed that the famous prognostic markers p53 and Ki-67 cannot distinguish NNF-PAs from INF-PAs either, indicating the demand for developing the novel molecular biomarkers.

Verification of the purified exosomes

Electron microscopy showed that the purified exosome was a tea saucer-like structure of 30-150 nm in size with distinct membrane (**Figure 1A**). Nanoparticle tracking analysis used to display the size and quantity of the exosomes indicated that nearly all recovered nanoparticles' diameters were less than 300 nm, with most of them in the range of 100-150 nm (**Figure 1B**).

CDK6 and RHOU were highly expressed in INF-PAs

We next performed ddPCR to detect the mRNA copy

Table 2. Clinicopathological features of NNF-PA and INF-PA patients included in the study

Groups	*n*	Age§ (yrs)	Gender (male/female, *n*)	p53 (*n*)		Ki-67 (*n*)		Largest diameter§ (mm)	Tumor texture (*n*)		
				Negative	Positive	⩽3%	>3%		Hard	Soft	Other
NNF	32	47.28±16.30	13/19	30	2	27	5	21.19±7.68	9	21	2
INF	14	47.86±17.09	6/8	14	0	10	4	30.34±7.70	3	9	2
t/χ^2 value		0.1095[a]	0.0200[b]	0.0292[b]		0.3777[b]		3.7152[a]	NA		
P value		>0.9999[a]	0.8875[b]	0.8644[b]		0.5388[b]		0.0006[a]	0.7717[c]		

§: Plus-minus values are means±SD.

NNF: noninvasive NF-PAs; INF: invasive NF-PAs; NA: not available.

[a] Unpaired *t* test; [b] *Chi-square* test; [c] *Fisher* test.

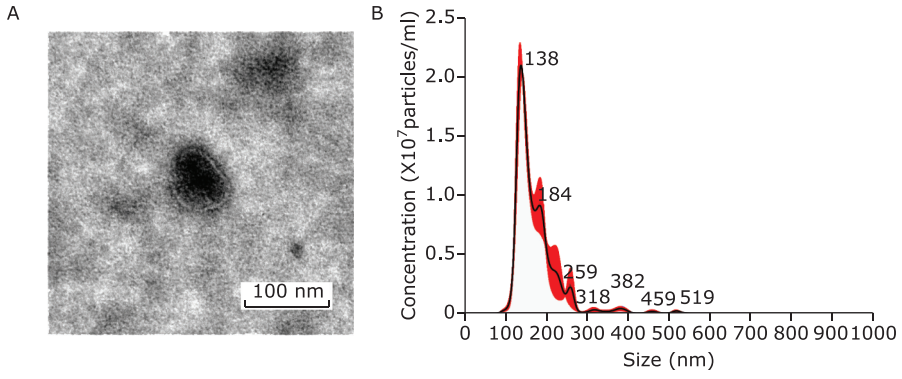

Figure 1. Validation of the exosomes recovered from the serum.

A. Representative electron microscopy picture of the purified exosome taken using negative staining method. B. Size distribution and concentration of the exosomes analyzed by NanoSight NS300 instrument.

number variations of candidate genes in exosomes. Less than 3 ng exosomal total RNA was purified and subsequently subjected to reverse transcription. To eliminate the significant difference in the total amount of RNA input among different patients which induced by amount of serum exosomes, the copy number of GAPDH was adopted as a reference control to exclude such effects. Of note, we rarely detected SPIRE2 mRNA, suggesting that SPIRE2 was not a good exosome biomarker for NF-PAs. After normalized to GAPDH, both CDK6 and RHOU showed significantly higher relative expression in INF-PAs as compared to NNF-PAs (CDK6: 0.2600±0.0912 *vs*. 0.1789±0.0628, $t=3.431$, $P=0.0013$; RHOU: 0.2696±0.1118 *vs*. 0.1788±0.0857, $t=2.946$, $P=0.0052$; **Figure 2**), suggesting these two molecules might be used to discriminate between NNF-PAs and INF-PAs.

CDK6 and RHOU can be used to discriminate INF-PAs from NNF-PAs

To evaluate the performance of CDK6 and RHOU as diagnostic indexes for INF-PAs, their diagnostic ability was analyzed by ROC curves. The AUC of CDK6 was 0.772 [95% confidence interval (*CI*): 0.600-0.943, $P=0.005$], and the AUC of RHOU was 0.757 (95% *CI*: 0.599-0.915, $P=0.007$), respectively (**Figure 3A**). We then calculated the cut-off points for CDK6 and RHOU to predict their ability in discriminating the invasiveness of NF-PAs. For CDK6 (cut-off score=0.2146), the accuracy, sensitivity, specificity and precision were 77.27%, 83.33%, 75.00% and 55.56%; similarly, the accuracy, sensitivity, specificity and precision for RHOU (cut-off score=0.1857) were 72.73%, 83.33%, 68.75% and 50.00%. These data collectively supported that both CDK6 and RHOU could be used as accurate and sensitive biomarkers to differ INF-PAs from NNF-PAs, although the precision was about 50%.

Additionally, we found that the mRNA levels of CDK6 and RHOU in serum exosomes were significantly positively correlated (Pearson correlation coefficient =0.935) (**Figure 3B**), suggesting they may be simultaneously involved in relevant biological network to initiate or promote the invasion of NF-PAs. To investigate their potential overlapped pathways, we queried "CDK6 AND RHOU" on KOBAS and GSEA, which turned out that these two genes were mainly co-regulating cell cycle-related processes. The top 20 enrichment pathways on KOBAS are shown in **Table 3**, including all 9 pathways revealed by GSEA marked as highlighted. The accordance of CDK6 and RHOU suggested that they might be used together for diagnosis. Indeed, after setting the double cut-off scores (0.2146 for CDK6 and 0.1857 for RHOU) as invasiveness threshold, we observed the elevated accuracy (81.82%), sensitivity (83.33%), specificity (81.25%) and precision (62.50%) (**Table 4**). These results indi-

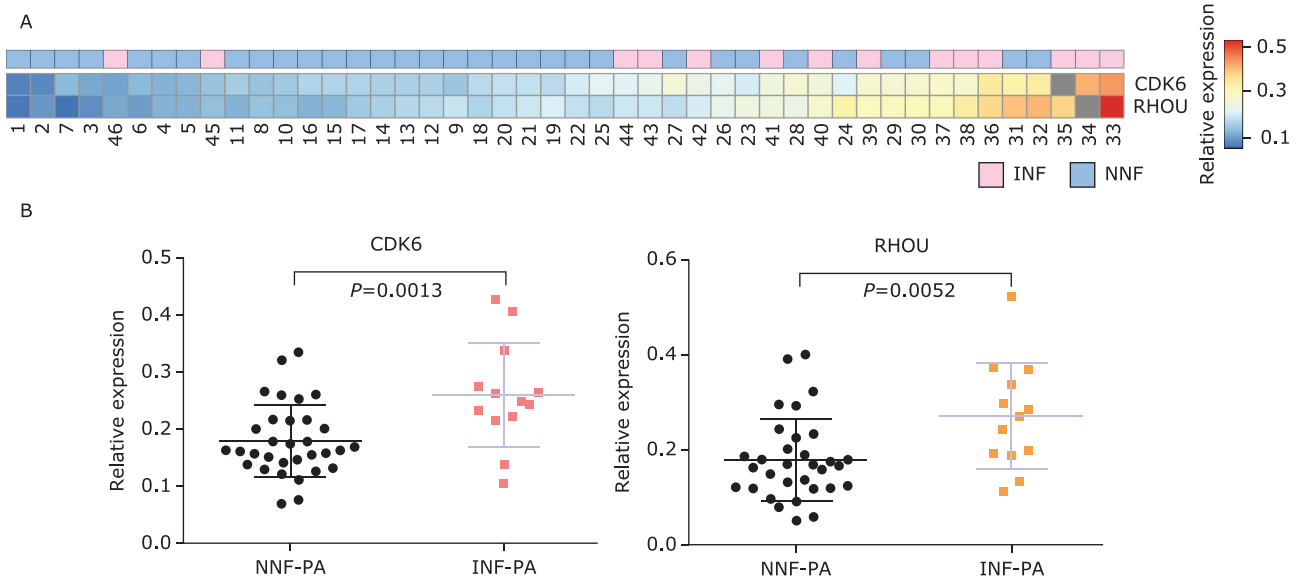

Figure 2. Differential expression of CDK6 and RHOU in exosomes from NF-PAs.

A. Heatmap of relative CDK6 and RHOU mRNA expression (normalized to GAPDH) in NNF-PAs and INF-PAs. Blocks filled with gray indicated the missing values. B. Statistical analysis of exosomal CDK6 and RHOU mRNA relative expression in NNF-PAs ($n=32$) compared with INF-PAs ($n=13$) samples. Data are shown as means±SD, compared with Unpaired *t* test.

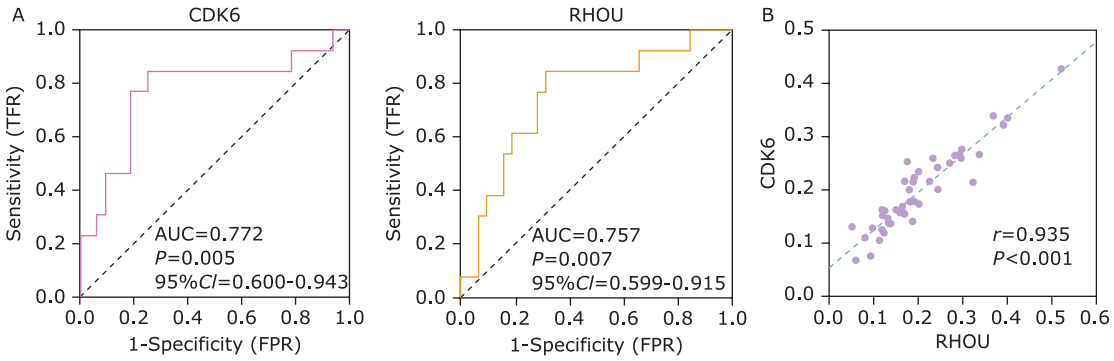

Figure 3. The evaluation of performance using CDK6 or RHOU to discriminate INF-PAs from NNF-PAs.
A. Receiver Operator Characteristic (ROC) curve of using CDK6 and RHOU exosomal mRNAs level to distinguish NNF-PAs from INF-PAs. B. The expressions of these two mRNAs in NF-PAs were prominently linear correlated.

Table 3. Functional enrichments of CDK6 and RHOU

Items	Database	ID	Background number	Corrected *P*-value	Input (gene ID)
G1/S transition of mitotic cell cycle	Gene Ontology	GO:0000082	230	0.0071	58480|1021
Cell cycle G1/S phase transition	Gene Ontology	GO:0044843	240	0.0071	58480|1021
Mitotic cell cycle phase transition	Gene Ontology	GO:0044772	447	0.0136	58480|1021
Cell cycle phase transition	Gene Ontology	GO:0044770	473	0.0136	58480|1021
Mitotic cell cycle process	Gene Ontology	GO:1903047	867	0.0182	58480|1021
Mitotic cell cycle	Gene Ontology	GO:0000278	937	0.0182	58480|1021
Cell cycle process	Gene Ontology	GO:0022402	1299	0.0182	58480|1021
Cytoskeletal part	Gene Ontology	GO:0044430	1468	0.0182	58480|1021
Cell cycle	Gene Ontology	GO:0007049	1665	0.0182	58480|1021
Cell projection	Gene Ontology	GO:0042995	1772	0.0182	58480|1021
Purine ribonucleoside triphosphate binding	Gene Ontology	GO:0035639	1788	0.0182	58480|1021
Purine ribonucleoside binding	Gene Ontology	GO:0032550	1798	0.0182	58480|1021
Ribonucleoside binding	Gene Ontology	GO:0032549	1801	0.0182	58480|1021
Purine nucleoside binding	Gene Ontology	GO:0001883	1801	0.0182	58480|1021
Nucleoside binding	Gene Ontology	GO:0001882	1808	0.0182	58480|1021
Purine ribonucleotide binding	Gene Ontology	GO:0032555	1830	0.0182	58480|1021
Purine nucleotide binding	Gene Ontology	GO:0017076	1843	0.0182	58480|1021
Ribonucleotide binding	Gene Ontology	GO:0032553	1846	0.0182	58480|1021
Cytoskeleton	Gene Ontology	GO:0005856	1983	0.0197	58480|1021

The top 20 Functional enrichment entries of CDK6 (gene ID: 1021) and RHOU (gene ID: 58480) on KOBAS. The result items on GSEA were highlighted. *P* values were corrected by false discovery rate (FDR) method.

cated that the combining CDK6 and RHOU were more powerful to distinguish INF-PAs from NNF-PAs.

DISCUSSION

It is known that intraoperative observation combined with postoperative recurrence are still the standard to define INF-PAs. No direct correlation was found between clinical features including age and gender, or biomarkers such as p53 and Ki-67 and the invasiveness of NF-PAs in this study. In many different tumors, p53 immunoreactivity or Ki-67 proliferative index > 3% facilitates the diagnosis or identification of tumor aggressiveness. However, the inconsistent results for Ki-67 and p53 activity in PAs were observed by different studies.[13, 14] In addition, histological features of p53 and Ki-67 were unable to distinguish benign or invasive PAs.[15, 16] To develop invasive and robust diagnostic biomarkers, we analyzed the absolute mRNA quantity of several potential cancer related genes in patients' serum exosomes based on our previous findings. Among these genes, both CDK6 and RHOU were

Table 4. Comparisons of the performance using CDK6, RHOU or both to distinguish between NNF-PAs and INF-PAs

Items	CDK6	RHOU	Combination
Total	44	44	44
Positives (P, *n*)	12	12	12
Negatives (N, *n*)	32	32	32
True positives (TP, *n*)	10	10	10
False positives (FP, *n*)	8	10	6
False negatives (FN, *n*)	2	2	2
True negatives (TN, *n*)	24	22	26
Accuracy (%)	77.27	72.73	81.82
Sensitivity (%)	83.33	83.33	83.33
Specificity (%)	75.00	68.75	81.25
Precision (%)	55.56	50.00	62.50

Accuracy (%) = (TP+TN)/Total × 100%, Sensitivity (%) = TP/P × 100%, Specificity (%) = TN/N × 100%, Precision (%) = TP/(TP+FP) × 100%.

significantly up-regulated in the INF-PAs group as compared to NNF-PAs and their variations were significantly positively correlated with each other.

Cyclin-dependent kinases (CDKs) are a family of serine-threonine kinases which play critical roles in orchestrating G1 phase progression and G1/S transition in cell cycle.[17] It is well studied that CDK6 is an over-expressed oncogenic gene in cancer cells and regulates the progression of many cancers, including medulloblastoma, malignant glioma, glioblastoma, lymphoma, hematopoietic malignancies, and cancers of pancreas, prostate, bladder.[18-25] Rho GTPases affect cell morphology, division, adhesion, motility, and contribute to migration and invasion of cancer cells, such as melanoma cells, breast carcinoma.[26-30] As a member of the Rho family of GTPases, RHOU (ras homolog family member U) has been identified to control cell migration in both multiple myeloma and acute lymphoblastic leukemia.[31, 32]

The higher expression of CDK6 and RHOU in INF-PAs indicated their important functions in the invasiveness of NF-PAs, and the underlying mechanism might be applied with other tumors. CDK6 has been recognized to play manifold roles in cancer progression, including promoting cell survival, proliferation and tumor growth *via* the retinoblastoma (Rb) protein.[18, 22, 23] RHOU has been reported as a response gene in Notch signaling in T-ALL cell[32] and in JAK/STAT pathway in multiple myelomas,[31] it can also cooperate with p21 activated kinase (PAK) family[32-35] to increase cell migration and/or adhesion. Notably, enhanced cell proliferation, migration and adhesion could trigger invasion. Besides, the remarkable positive expression correlation of these two genes suggested they might be involved in one regulatory network, for example, they both regulate cell cycle. Canovas Nunes *et al*.[31] had observed a significant cell cycle arrest at G1/S phase transition in response to RHOU silencing, which further support that RHOU and CDK6 might interact with each other in tumors development (Table 3). In a word, it is speculated that CDK6 and RHOU have both unique and overlapping mechanisms in the invasion of NF-PAs. Further investigations revealing the detail molecular mechanism of both CDK6 and RHOU regulating NF-PAs development may expand our understanding of the pathogenesis and invasiveness of NF-PAs and thus improve postoperative management.

The important roles of CDK6 and RHOU drove us to explore their capacity as biomarkers. Strikingly, using the individual cut-off score of CDK6 or RHOU could already distinguish INF-PAs from NNF-PAs with high sensitivity and accuracy. More importantly, combination of these two biomarkers could significantly improve the specificity and precision to diagnose INF-PAs or NNF-PAs. Further studies with more biomarkers and validation in a larger cohort are required to improve the diagnostic panels.

Taken together, our study identified CDK6 and RHOU can be used as blood-based circulating biomarkers to discriminate between INF-PAs and NNF-PAs, which is also helpful to predict prognosis and develop accurate postoperative treatment for these patients. As single molecule is insufficient to determine tumor subtypes, the combination of several molecules may be a straightforward strategy to establish a better diagnostic system.

Conflicts of interest statement

All authors declare no conflicts of interest.

REFERENCES

1. Asa SL, Ezzat S. The cytogenesis and pathogenesis of pituitary adenomas. Endocr Rev 1998; 19(6):798-827. doi: 10.1210/edrv.19.6.0350.
2. Daly AF, Rixhon M, Adam C, et al. High prevalence of pituitary adenomas: a cross-sectional study in the

province of Liege, Belgium. J Clin Endocrinol Metab 2006; 91(12):4769-75. doi: 10.1210/jc.2006-1668.
3. Fernandez A, Karavitaki N, Wass JA. Prevalence of pituitary adenomas: a community-based, cross-sectional study in Banbury (Oxfordshire, UK). Clin Endocrinol (Oxf) 2010; 72(3):377-82. doi: 10.1111/j.1365-2265.2009.03667.x.
4. Lopes MBS. The 2017 World Health Organization classification of tumors of the pituitary gland: a summary. Acta Neuropathol 2017; 134(4):521-35. doi: 10.1007/s00401-017-1769-8.
5. Selman WR, Laws ER, Jr., Scheithauer BW, et al. The occurrence of dural invasion in pituitary adenomas. J Neurosurg 1986; 64(3):402-7. doi: 10.3171/jns.1986.64.3.0402.
6. Thapar K, Kovacs K, Scheithauer BW, et al. Proliferative activity and invasiveness among pituitary adenomas and carcinomas: an analysis using the MIB-1 antibody. Neurosurgery 1996; 38(1):99-106; discussion 106-7. doi: 10.1097/00006123-199601000-00024.
7. Raverot G, Burman P, McCormack A, et al. European Society of Endocrinology Clinical Practice Guidelines for the management of aggressive pituitary tumours and carcinomas. Eur J Endocrinol 2018; 178(1):G1-g24. doi: 10.1530/eje-17-0796.
8. Boriachek K, Islam MN, Moller A, et al. Biological functions and current advances in isolation and detection strategies for exosome nanovesicles. Small 2018; 14(6). doi: 10.1002/smll.201702153.
9. Vlassov AV, Magdaleno S, Setterquist R, et al. Exosomes: current knowledge of their composition, biological functions, and diagnostic and therapeutic potentials. Biochim Biophys Acta 2012; 1820(7):940-8. doi: 10.1016/j.bbagen.2012.03.017.
10. Del Re M, Biasco E, Crucitta S, et al. The detection of androgen receptor splice variant 7 in plasma-derived exosomal RNA strongly predicts resistance to hormonal therapy in metastatic prostate cancer patients. Eur Urol 2017; 71(4):680-7. doi: 10.1016/j.eururo.2016.08.012.
11. Knosp E, Steiner E, Kitz K, et al. Pituitary adenomas with invasion of the cavernous sinus space: a magnetic resonance imaging classification compared with surgical findings. Neurosurgery 1993; 33(4):610-7; discussion 7-8. doi: 10.1097/00006123-199310000-00008
12. Corbisier P, Pinheiro L, Mazoua S, et al. DNA copy number concentration measured by digital and droplet digital quantitative PCR using certified reference materials. Anal Bioanal Chem 2015; 407(7):1831-40. doi: 10.1007/s00216-015-8458-z.
13. Asa SL, Ezzat S. The pathogenesis of pituitary tumors. Annu Rev Pathol 2009; 4(1):97-126. doi: 10.1146/annurev.pathol.4.110807.092259.
14. Sav A, Rotondo F, Syro LV, et al. Biomarkers of pituitary neoplasms. Anticancer Res 2012; 32(11):4639-54.
15. Amar AP, Hinton DR, Krieger MD, et al. Invasive pituitary adenomas: significance of proliferation parameters. Pituitary 1999; 2(2):117-22.
16. Knosp E, Kitz K, Perneczky A. Proliferation activity in pituitary adenomas: measurement by monoclonal antibody Ki-67. Neurosurgery 1989; 25(6):927-30. doi: 10.1227/00006123-198912000-00012
17. Zhao X, Li J, Huang S, et al. MiRNA-29c regulates cell growth and invasion by targeting CDK6 in bladder cancer. Am J Transl Res 2015; 7(8):1382-9.
18. Mendrzyk F, Radlwimmer B, Joos S, et al. Genomic and protein expression profiling identifies CDK6 as novel independent prognostic marker in medulloblastoma. J Clin Oncol 2005; 23(34):8853-62. doi: 10.1200/jco.2005.02.8589.
19. Costello JF, Plass C, Arap W, et al. Cyclin-dependent kinase 6 (CDK6) amplification in human gliomas identified using two-dimensional separation of genomic DNA. Cancer Res 1997; 57(7):1250-4.
20. Bax DA, Mackay A, Little SE, et al. A distinct spectrum of copy number aberrations in pediatric high-grade gliomas. Clin Cancer Res 2010; 16(13):3368-77. doi: 10.1158/1078-0432.Ccr-10-0438.
21. Nagel S, Leich E, Quentmeier H, et al. Amplification at 7q22 targets cyclin-dependent kinase 6 in T-cell lymphoma. Leukemia 2008; 22(2):387-92. doi: 10.1038/sj.leu.2405028.
22. Nebenfuehr S, Bellutti F, Sexl V. Cdk6: at the interface of Rb and p53. Mol Cell Oncol 2018; 5(5):e1511206. doi: 10.1080/23723556.2018.1511206.
23. Lee KH, Lotterman C, Karikari C, et al. Epigenetic silencing of MicroRNA miR-107 regulates cyclin-dependent kinase 6 expression in pancreatic cancer. Pancreatology 2009; 9(3):293-301. doi: 10.1159/000186051.
24. Lim JT, Mansukhani M, Weinstein IB. Cyclin-dependent kinase 6 associates with the androgen receptor and enhances its transcriptional activity in prostate cancer cells. Proc Natl Acad Sci U S A 2005; 102(14):5156-61. doi: 10.1073/pnas.0501203102.
25. Wang G, Zheng L, Yu Z, et al. Increased cyclin-depen-

dent kinase 6 expression in bladder cancer. Oncol Lett 2012; 4(1):43-6. doi: 10.3892/ol.2012.695.
26. Symons M, Segall JE. Rac and Rho driving tumor invasion: who's at the wheel? Genome Biol 2009; 10(3):213. doi: 10.1186/gb-2009-10-3-213.
27. Liu S, Wang Y, Xue W, et al. Genetic variants in the genes encoding rho GTPases and related regulators predict cutaneous melanoma-specific survival. Int J Cancer 2017; 141(4):721-30. doi: 10.1002/ijc.30785.
28. Vega FM, Ridley AJ. Rho GTPases in cancer cell biology. FEBS Lett 2008; 582(14):2093-101. doi: 10.1016/j.febslet.2008.04.039.
29. Parri M, Chiarugi P. Rac and Rho GTPases in cancer cell motility control. Cell Commun Signal 2010; 8(1):23. doi: 10.1186/1478-811x-8-23.
30. Simpson KJ, Dugan AS, Mercurio AM. Functional analysis of the contribution of RhoA and RhoC GTPases to invasive breast carcinoma. Cancer Res 2004; 64(23):8694-701. doi: 10.1158/0008-5472.Can-04-2247.
31. Canovas Nunes S, Manzoni M, Pizzi M, et al. The small GTPase RhoU lays downstream of JAK/STAT signaling and mediates cell migration in multiple myeloma. Blood Cancer J 2018; 8(2):20. doi: 10.1038/s41408-018-0053-z.
32. Bhavsar PJ, Infante E, Khwaja A, et al. Analysis of Rho GTPase expression in T-ALL identifies RhoU as a target for Notch involved in T-ALL cell migration. Oncogene 2013; 32(2):198-208. doi: 10.1038/onc.2012.42.
33. Dart AE, Box GM, Court W, et al. PAK4 promotes kinase-independent stabilization of RhoU to modulate cell adhesion. J Cell Biol 2015; 211(4):863-79. doi: 10.1083/jcb.201501072.
34. Hodge RG, Ridley AJ. Regulation and functions of RhoU and RhoV. Small GTPases 2017; 30:1-8. doi: 10.1080/21541248.2017.1362495.
35. Faure S, Fort P. Atypical RhoV and RhoU GTPases control development of the neural crest. Small GTPases 2015; 6(4):174-7. doi: 10.1080/21541248.2015.1025943.